Guiding of High Intensity Laser Pulses in Straight and Curved Plasma Channel Experiments

Y. Ehrlich, C. Cohen, and A. Zigler
Racah Institute of Physics, Hebrew University, Jerusalem, Israel

J. Krall, P. Sprangle, and E. Esarey
Beam Physics Branch, Plasma Physics Division, Naval Research Laboratory, Washington, D.C. 20375
(Received 30 July 1996)

Experimental demonstration of optical guiding of a high intensity ($>10^{16}$ W/cm^2) laser pulse in a 1 cm long cylindrical plasma channel formed by a slow capillary discharge is presented. Optical guiding in a curved plasma (radius of curvature = 10 cm) is also demonstrated. It is shown experimentally that the guiding mechanism is insensitive to laser intensity over a wide range ($\sim 10^8 - 10^{16}$ W/cm^2). Results show guiding over $\simeq 11$ vacuum diffraction lengths in both straight and curved channels, in agreement with theory and simulation. [S0031-9007(96)01625-0]

PACS numbers: 52.40.Nk

Laser guiding in straight and curved plasma channels can have important applications, such as an efficient x-ray laser medium, optical synchrotrons, laser accelerators, and harmonic generators [1–5]. Generally, laser propagation distance is limited by diffraction and can be further limited by ionization-induced refraction [6,7]. Hence optical guiding is needed. One approach to optical guiding of intense pulses relies on the self-induced modification of the plasma refractive index due to relativistic electron motion [8] or by ponderomotive force-driven charge displacement [9]. Another approach to guiding relies on a preformed plasma density channel in which the refractive index is peaked on axis by minimizing the local ambient electron density on axis [10]. Guiding in a preformed plasma channel has been demonstrated previously [11,12] using moderate intensity ($>10^{15}$ W/cm^2) laser pulses. In these experiments, a first pulse initiates a cylindrical expanding shock wave in a gas chamber to form a straight plasma channel, which guides a second pulse over distances as large as 90 laser diffraction lengths [12]. Initial experiments on the guiding of laser pulses in one-dimension using a slab geometry capillary discharge have also been reported [13].

In this Letter we report the optical guiding of a high intensity ($>10^{16}$ W/cm^2) laser pulse over several vacuum diffraction (Rayleigh) lengths using a plasma channel formed by a slow electrical discharge in a cylindrical capillary. Using this technique, we have obtained the first demonstration of guiding along a curved channel.

In these experiments, guiding took place for intensities varying from $\sim 10^8$ W/cm^2 (using the oscillator only) to greater than 10^{16} W/cm^2. Results are consistent with the theoretical prediction that density channel guiding is a first-order process, independent of laser intensity [10]. The temperature and plasma density near the capillary axis can be modified over a wide range [14], independent of guiding conditions (channel absolute depth and width). The formation of a highly localized plasma channel by a capillary discharge in a vacuum cell enables focusing of high intensity laser pulses at the channel entrance and avoids laser propagation in a neutral gas before the laser focus. The generated plasma consists of ions of the capillary wall material, which is made of a compound with a high concentration of hydrogen. Thus the effective ionization state in the plasma remains almost constant even for very high laser intensities.

The experimental configuration is shown in Fig. 1. A 1 cm long polypropylene cylinder with a 350 μm diameter hole is placed between two electrodes. The electrodes are connected to an 11 nF capacitor which is charged to 0.2–0.5 J. The discharge, which is initiated by a triggered spark-gap, has a maximum repetition rate of 1.5 Hz. The energy stored in the capacitor is ohmically dissipated in the capillary discharge and transfers energy from the capacitor to the plasma with high efficiency. This energy is partitioned between plasma pressure, dissociation, and ionization energy, as well as kinetic energy of the plasma flow. Under conditions where the flow kinetic energy is smaller than the thermal energy, the balance between the power radiated by the plasma and input electrical power define experimentally verified scaling rules for the plasm temperature T, capillary resistance R, and plasma density n as functions of the capillary geometry and the current I [14]: $T = 3.3I^{0.36}$ eV, $n = 1.3 \times 10^{20} I^{0.91}$ cm^{-3}, and $R = 1.71I^{-0.55}$ Ω, where I is in kA. Thus the capillary

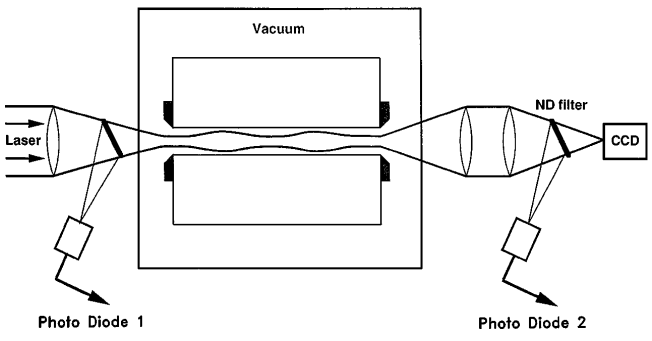

FIG. 1. Experimental setup.

 0031-9007/96/77(20)/4186(4)$10.00

plasma can be controlled by varying the parameters of the external circuit.

For experiments in which the capillary radius was smaller than Rosseland [15] mean free path, which governs the radiation losses, the plasma pressure and temperature are such that the radial electron density profile was found to be parabolic, with a minimum on axis [16]. Specifically, the pressure across the capillary is constant, since any disturbance in the radial direction equilibrates on a time scale much shorter than both the discharge duration ($\sim 1\ \mu$s) and the plasma flow time along the channel. In addition, the temperature is higher at the center and drops near the wall, due to radiation and collisional heat transfer. In this experiment and in Ref. [16], the axial plasma temperature was ~ 3 eV and the electron density varied within the range $\sim(1-5) \times 10^{19}$ cm^{-3}.

For a parabolic plasma channel of the form $n = n_0 + \Delta n r^2/r_{\rm ch}^2$, where $r_{\rm ch}$ is the radius of the plasma channel, it can be shown [10] that a laser pulse with a radial profile $\sim\exp(-r^2/r_L^2)$ will be matched ($dr_L/dz = 0$) within the channel with a laser spot size (radius) $r_L = r_M$ given by $r_M = [r_{\rm ch}^2/(\pi r_e \Delta n)]^{1/4}$, where $r_e = e^2/mc^2$ is the classical electron radius. For representative parameters $r_{\rm ch} = 150\ \mu$m and $n_0 \simeq \Delta n = 4 \times 10^{18}$ cm^{-3}, the matched beam radius is $r_M = 28\ \mu$m.

Both a 1 cm long straight capillary tube with an inner diameter of 350 μm, as well as a curved capillary tube, with length 1 cm, inner diameter 350 μm, and radius of curvature 10 cm, were used. The experiments were conducted using the Hebrew University Laser which consists of a Ti-Sapphire oscillator followed by regenerative and four-pass amplifiers. The system is capable of delivering a linearly-polarized, 100 fs pulse with energy up to 50 mJ at wavelength $\lambda = 0.80\ \mu$m with repetition rate of 10 Hz. Timing electronics allow synchronization of the laser pulse arrival and the discharge initiation with a variable delay.

The laser was focused on the capillary channel by means of an $F^{\#} = 11.5$ lens, which produces a laser waist $r_{L0} \simeq 15\ \mu$m when focused in vacuum. The minimum spot size of 15 μm implies that the beam is ~ 1.6 times the diffraction-limited value of $\lambda F^{\#} \simeq 9.2\ \mu$m [17]. Operating at pulse energy 4 mJ, the peak focused intensity was $\sim 10^{16}$ W/cm^2. The capillary was located in a 10^{-4} torr vacuum chamber, with the capillary entrance placed at the focal plane of the laser focusing lens. Alignment was achieved using a 1 mW He-Ne laser and the Ti-Sapphire oscillator.

The input and transmitted laser energy in the capillary was measured by splitting and focusing a portion of the beam into two calibrated photo diodes (see Fig. 1). Photo diode 1 provides input data, including laser energy and timing. Photo diode 2 measures the amount of laser light transmitted through the capillary. The laser light transmitted through the plasma channel was collected and imaged onto a CCD camera. The imaged intensity was reduced by inserting thin calibrated neutral density filters. Figures 2 and 3 show single-shot images of the laser beam at the capillary exit, recorded at 10 Hz by the CCD camera with and without the discharge for the straight (Fig. 2) and curved (Fig. 3) capillary tubes. The difference between the maximum discharge repetition rate (1.5 Hz) and laser repetition rate (10 Hz) allows comparison of the guided and unguided laser pulse images under otherwise identical conditions. Figures 2 and 3 show guiding over a distance $\simeq 11 Z_{R0}$, where $Z_{R0} = \pi r_{L0}^2/\lambda = 0.088$ cm is the Rayleigh length.

The laser beam expansion after passing through the capillary channel was measured by recording the images of the transmitted light at various locations. Measurements were taken at distances between 0 and 1 cm from the capillary exit. In the case of the straight capillary, the focusing and collecting optics were placed on the same optical axis. In the curved capillary experiments the optical systems were placed at an angle of 3° relative to the channel axis (6° between the two optical systems axes).

Experimental results show substantial increases in the laser energy transmission and a substantial reduction of the laser spot size at the capillary exit when the capillary is discharged. When the laser pulse (focused using an $F^{\#} = 11.5$ lens) was transmitted through the straight capillary without an electrical discharge, the energy transmission was 25%. This value corresponds to the geometrical opening of the capillary and indicates very low reflection at the capillary walls. When the pulse is focused at the capillary entrance 250 ns after initiation of the electrical discharge, the typical energy transmission increases to 75% and the emerging pulse radius is reduced to 30 μm (Fig. 2). Experimental results indicate a critical

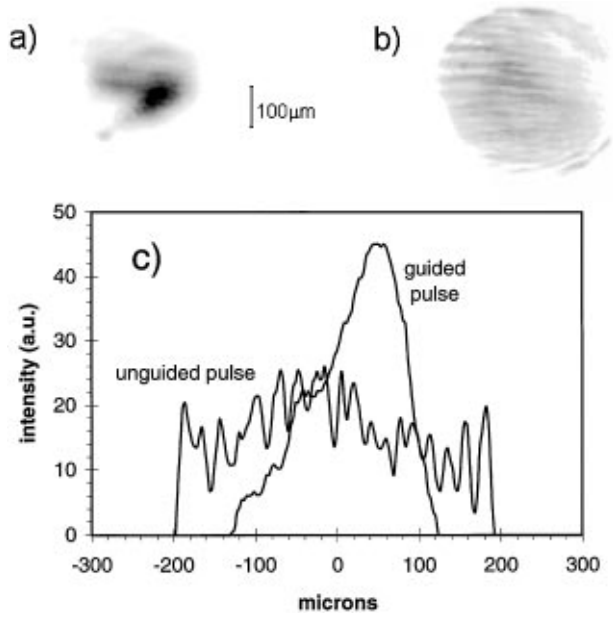

FIG. 2. CCD images of the laser pulse emerging from the straight capillary for (a) a guided pulse and (b) an unguided pulse. Intensity profiles (c) are also shown. Note that the focal plane is 2 mm from the capillary exit and that the interference lines are due to low grade neutral density filters.

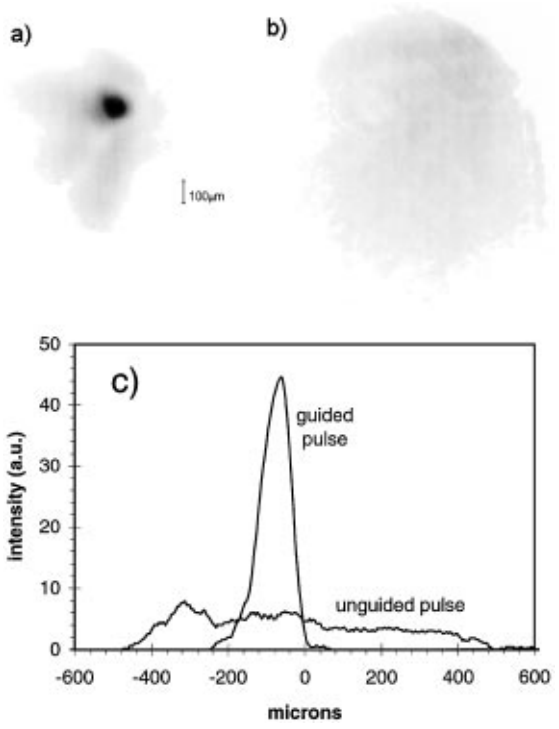

FIG. 3. CCD images of the laser pulse emerging from the curved capillary (radius of curvature 10 cm) for (a) a guided pulse and (b) an unguided pulse. Intensity profiles (c) are also shown. The focal plane is 5 mm from the capillary exit.

sensitivity to alignment and timing between initiation of the discharge and the arrival of the laser pulse. Enhanced capillary transmission is obtained for laser pulses injected 200 to 350 ns after the discharge is initiated. For shorter delays, no significant effect was observed. For longer delays, the spot size of the transmitted pulse remains small (as in optimal case), but the amount of the transmitted light is reduced.

Performance as a function of stored electrical energy was studied in the straight capillary geometry by using two capacitors for the electrical discharge : 2.1 and 11 nF and by varying the voltage across the capillary. However, voltage variation also affects the plasma density according to the scaling rules stated earlier. Optimal guiding was obtained using the 2.1 nF capacitor and a discharge voltage of 13 kV. For these values, the maximum current was 500 A. Using the 2.1 nF capacitor, capillary wall erosion was small, with no significant widening of the capillary channel after 100 shots. For discharge voltages significantly above 15 kV, the transmitted laser intensity was negligible; at low voltages, the guiding was less pronounced. Measurements of the beam diameter at various distances from the capillary exit were obtained by varying the distance between the capillary exit and the focal plane of the collecting optical system. It was found that the laser spot size did not vary significantly at distances from 2 to 7 mm away from the capillary exit. Small shot-to-shot variations in the spot size were attributed to variations in Δn consistent with simulation results. In addition, plane imaging was used to measure the beam profile at several positions after the exit of the capillary tube in the same shot. For this purpose, five beam splitters were placed between the imaging lens and the CCD camera. The image taken by each beam splitter shows the laser radial profile at a particular position. Beam profile data were taken at distances 0, 0.2, 0.4, 0.6, and 0.8 cm from the exit of the capillary. A divergence angle of $\gtrsim 8$ mrad was found.

Figure 3 shows the results of optical guiding experiments along a curved plasma channel using the 11 nF capacitor and a discharge voltage of 9.3 kV. In the curved channel experiments, capillary performance was sensitive to the alignment of the laser beam with respect to the capillary axis. With optimal alignment and a 10 cm radius-of-curvature plasma channel, energy transmission was as high as 85%, and the laser spot radius at the capillary exit was 50 μm. In experiments using a capillary with a 4.2 cm radius of curvature (other parameters identical), the peak energy transmission was $\sim 2\%$, in good agreement with theory (see below).

To examine propagation of the laser pulse in the straight channel, simulations were performed using a 2D (r, z) nonlinear fluid code [18]. Figure 4 shows the laser spot radius r_L plotted versus propagation distance z through the channel, which is located at $0.5 < z < 1.5$ cm. In the simulation, the on-axis plasma density is 5.0×10^{18} cm^{-3}, $\Delta n = 4.0 \times 10^{18}$ cm^{-3}, and $r_{\rm ch} = 150$ μm. The laser pulse is focused at the channel entrance with a minimum spot size $r_{L0} = 15$ μm. Since the experimental spot size is 1.6 times the diffraction-limited value, the simulation code was heuristically modified to reduce the vacuum diffraction length by this same factor. Figure 4 shows that the laser spot radius oscillates about the matched beam radius $r_M = 28$ μm as it is guided through the 1 cm long channel. For comparison to the guided case, laser propagation in vacuum (no channel) is also shown. At the capillary exit, the laser spot radius is 45 μm and the divergence angle is $\simeq 14$ mrad, in good agreement with experiment.

Laser propagation in a curved plasma channel can be analyzed in the low-intensity limit, in which, nonlinear (relativistic and ponderomotive) effects are neglected and the channel is unaffected by the laser. In a straight channel, the laser electric field $E = \frac{1}{2}\hat{E}e^{ik(z-ct)} + \text{c.c.}$ obeys the paraxial wave equation

$$(\nabla_\perp^2 + 2ik\partial/\partial z)\hat{E} = k^2(1 - \eta^2)\hat{E}\,, \qquad (1)$$

where $\omega = ck$ is the laser frequency, z is along the channel axis, η is the index of refraction, c.c. denotes the complex conjugate, and $|\partial\hat{E}/\partial z| \ll k|\hat{E}|$ is assumed. The linear index of refraction for a plasma is given by $\eta \simeq 1 - \omega_p^2/2\omega^2$, where $\omega_p = (4\pi e^2 n/m)^{1/2}$ is the plasma frequency and n is the plasma density.

Consider a channel which is curved in the (x, z) plane with a constant radius of curvature R_0, where z

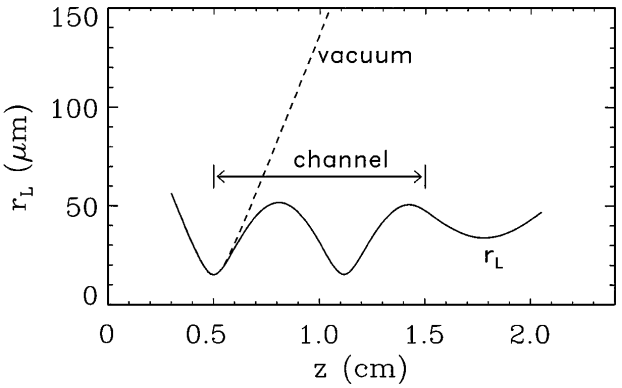

FIG. 4. Simulation result (solid line) showing laser spot radius r_L plotted versus propagation distance z. The channel is located at $0.5 < z < 1.5$ cm. For comparison, laser propagation in vacuum (no channel) is also shown.

is the distance along the curved channel axis, and $r = (x^2 + y^2)^{1/2}$ is defined with respect the channel axis. The paraxial wave operator in the curved coordinate system becomes $(\nabla_\perp^2 + 2ik\partial/\partial z + 2k^2 x/R_0)\hat{E}$ where $\nabla_\perp^2 = \partial^2/\partial x^2 + \partial^2/\partial y^2$ and higher order terms (smaller by at least $r/R_0 \ll 1$) have been neglected. Hence the laser field envelope $\hat{E}$ obeys the paraxial wave equation, Eq. (1), with an effective refractive index

$$\eta_{\text{eff}} = 1 - \omega_p^2(r)/2\omega^2 + x/R_0 , \qquad (2)$$

where the x/R_0 term represents the effects the curvature. Assuming a density channel of the form $n = n_0 + \Delta n r^2/r_{\text{ch}}^2$, it can be shown that the solution to Eq. (1) with $\eta = \eta_{\text{eff}}$ is given by

$$\hat{E} = E_0 \exp[i\Delta k z + ik_x(x - x_c) - (x - x_c)^2/r_0^2 - y^2/r_0^2] , \qquad (3)$$

where r_0 is the matched laser spot radius given by $r_0^4 = r_{\text{ch}}^2/\pi r_e \Delta n$, $\Delta k \ll k$ represents a small phase shift $k_x = k\partial x_c/\partial z$, and the laser pulse centroid x_c satisfies

$$\partial^2 x_c/\partial z^2 + x_c/Z_{R0}^2 = 1/R_o , \qquad (4)$$

where $Z_{R0} = kr_0^2/2$ is the Rayleigh length of the matched beam. Equation (4) indicates that the laser centroid x_c oscillates in z about an equilibrium offset value given by $x_{c0} = Z_{R0}^2/R_0$. Clearly this offset must be less than the channel radius or the laser will be lost from the channel. This sets a minimum acceptable radius of curvature:

$$R_0 \geq Z_{R0}^2/r_{\text{ch}} . \qquad (5)$$

For a matched beam ($r_0 = 28$ μm) and representative experimental parameters ($\lambda = 0.8$ μm and $r_{\text{ch}} = 150$ μm), $Z_{R0} = 0.31$ cm and $R_0 \geq 6.4$ cm. This value is in excellent agreement with the experimental results.

In summary, optical guiding of high intensity ($> 10^{16}$ W/cm^2) laser pulses has been demonstrated using both straight and curved channel geometries, where the plasma channel is formed by a slow cylindrical capillary discharge. Results demonstrate guiding of $\gtrsim 75\%$ of the laser pulse energy over a distance $\simeq 11$ Rayleigh lengths.

This work was supported by the U.S.-Israeli Binational Science Foundation, the U.S. Office of Naval Research, and the U.S. Department of Energy.

[1] See, e.g., Special Issue on Plasma Based Accelerators, edited by T. Katsouleas and R. Bingham [IEEE Trans. Plasma Sci. **24**, 249–460 (1996)]; C. E. Clayton *et al.*, Phys. Rev. Lett. **70**, 37 (1993); K. Nakajima *et al.*, Phys. Rev. Lett. **74**, 4428 (1995); A. Modena *et al.*, Nature (London) **337**, 606 (1995).
[2] P. Sprangle *et al.*, Appl. Phys. Lett. **53**, 2146 (1988); E. Esarey *et al.*, Phys. Fluids B **5**, 2690 (1993).
[3] H. Milchberg, C. Durfee, and J. Lynch, J. Opt. Soc. Am B **12**, 731 (1995).
[4] J. Macklin, J. Kmetec, and C. Gordon, Phys. Rev. Lett. **70**, 760 (1993).
[5] P. Eisenberger and S. Suckewer, Science (in press).
[6] P. Sprangle *et al.*, Phys. Rev. E (to be published).
[7] W. P. Leemans *et al.*, Phys. Rev. A **46**, 1091 (1992).
[8] C. E. Max, J. Arons, and A. B. Langdon, Phys. Rev. Lett. **33**, 209 (1974); P. Sprangle, C. M. Tang, and E. Esarey, IEEE Trans. Plasma Sci. **PS-15**, 145 (1987).
[9] G. Z. Sun *et al.*, Phys. Fluids **30**, 526 (1987); A. B. Borisov *et al.*, Phys. Rev. A **45**, 5830 (1992).
[10] P. Sprangle and E. Esarey, Phys. Fluids B **4**, 2241 (1992); P. Sprangle *et al.*, Phys. Rev. Lett. **69**, 2200 (1992); E. Esarey, J. Krall, and P. Sprangle, Phys. Rev. Lett. **72**, 2887 (1994).
[11] C. Durfee and H. Milchberg, Phys. Rev. Lett. **71**, 2409 (1993).
[12] H. M. Milchberg *et al.*, Phys. Plasmas **3**, 2149 (1996).
[13] A. Zigler *et al.*, J. Opt. Soc. Am. B **13**, 68 (1996).
[14] A. Loeb and Z. Kaplan, IEEE Trans. Magn. **25**, 342 (1989); R. Burton *et al.*, IEEE Trans. Plasma Sci. **19**, 340 (1991); Y. Ehrlich *et al.*, Appl. Phys. Lett. **64**, 3542 (1994).
[15] Ya. B. Zel'dovich and Yu. P. Razier, *Physics of Shock Waves and High Temperature Hydrodynamic Phenomena* (Academic Press, New York, 1966).
[16] J. Ashkenazy, R. Kipper, and M. Caner, Phys. Rev. A **43**, 5568 (1991); B. Brill *et al.*, J. Phys. D **23**, 1064 (1990); A. Loeb and Z. Kaplan, IEEE Trans. Magn. **25**, 342 (1989); E. Lithman, M.Sc. Thesis, Hebrew University, 1995.
[17] A. E. Seigman, *Lasers* (University Science Books, Mill Valley, California, 1986), p. 676.
[18] J. Krall *et al.*, Phys. Plasmas **1**, 1738 (1994).